Appl. Math. Inf. Sci. 7, No. 4, 1511-1517 (2013) 1511

Applied Mathematics & Information Sciences
An International Journal

http://dx.doi.org/10.12785/amis/070434

Identity Concealment of Brain Images by Masking

Ruoyu Du[1] *and Hyo Jong Lee*[1,2,*]

[1]Division of Computer Science and Engineering, Chonbuk National University, Jeonju, South Korea
[2]Center for Advanced Image and Information Technology, Chonbuk National University, Jeonju, South Korea

Received: 21 Dec. 2012, Revised: 11 Jan. 2013, Accepted: 13 Feb. 2013
Published online: 1 Jul. 2013

Abstract: In this paper, a novel method of concealment of facial information was proposed to protect the patient's privacy. It consists with two steps: the construction of a standard brain template and substitution of the template to a new brain image data. Fifteen medical brain images are used to build the standard brain template. Registration and normalization procedures are applied to construct the standard brain templates by using B-Spline registration. Segmentation is used to substitute the original image for the template image and brain extraction. Canny-edge Level set segmentation algorithm is applied to segment a scalp-skull part from a whole brain volume data. New medical brain images are substituted for the standard template to construct the anonymous face models. In order to verify the validity of the anonymous face model, volumes of extracted brains from an original test brain and its anonymous brain were compared. The result shows that the actual brain part from the anonymous brain is exactly same as one which comes from an original medical brain image.

Keywords: Anonymous face model, B-Spline registration, Level-set algorithm, Canny-edge detection

1 Introduction

Privacy protection of medical image has been an important issue when digital images and their pertinent patient information are transmitted across public networks. Mandates for ensuring health data security have been issued by the federal government such as Health Insurance Portability and Accountability Act (HIPAA), where healthcare institutions are obliged to take appropriate measures to ensure that patient information is only provided to people who have a professional need. For medical brain image dataset to qualify as sharable under the "safe harbor" regulations, one of the HIPAA-defined identifiers that must be removed is "full face photographic images and any comparable images" [1, 2]. With the increasing resolution of morph metric MR scans, it has become possible to reconstruct detailed images showing facial anatomy. Thus, in order to share unaltered MRI images, both sites are required to provide a waiver of consent. This becomes problematic in multifarious projects, particularly, those with the goal of making data available to a larger research community.

"Anonymous" means that the researcher can in no way identify the subjects. By using anonymity technology, identifying information is not being requested. There will be some specific situation in medical image processing. Suppose brain surgeons intend to analyze a patient's related information with 3D brain model, real face is bound to be recognized when 3D brain model is reconstructed. It is difficult to conceal these natural facial features, even if we just remove the patient identifiers. The most direct solution is to cover these facial features with something, such as a cylinder mask. Yet, this solution has a drawback: it is easy to separate the mask from the original image. A more recent approach has suggested combining multiple automated skull-stripping methods within a single meta-algorithm to optimize results [3]. Another concern is that many of these methods may remove certain elements, such as extra-cranial cerebrospinal fluid (CSF) [4], which hold some importance in some fields of research. With recent advances in combining MRI with EEG/MEG [5], cranial features are important for identifying electrode placement with respect to a structural MRI. These features would be removed when a skull-stripping algorithm is applied. Skull-stripping methodology, then, may not be sufficiently reliable for large-scale, automated de-identification purposes [6, 7, 8]. A defacing algorithm was developed that uses models of non-brain structures for removing potentially identifying facial features while

* Corresponding author e-mail: hlee@jbnu.ac.kr

preserving brain tissue for future analyses. Visual inspection of the defaced images showed none had brain tissue removed. In order to quantify the effects of defacing on a volume, the different datasets were bias corrected with N3 [9], defaced, and then skull-stripped using either a hybrid watershed algorithm [10] or Brain Surface Extractor [11,12]; previous study of skull-stripping algorithms suggested that these techniques may be the most adept at automated skull stripping for the pulse sequences and patient populations employed herein [13]. An additional consideration is whether this defacing algorithm can be suitable for most patients. Because it is hard to remove the special identifying facial features, these features can be recognized in the forehead.
Therefore an anonymous face model of medical brain imaging proposed in this paper, which is a novel challenge to protect individual privacy. The patient's face will be replaced by a non-recognized face. However, the patient's brain information is still intact. This method can hide the personal information well to protect the privacy of the patient. In this paper, an anonymous face model is completed by building a standard brain template without the brain part and combining a test medical brain image. In addition, an improvement scalp-skull-stripping algorithm is applied named "Canny-edge Level-Set" segmentation method. The rest of the paper is organized as follows. Section 2 is devoted to materials and methods. Section 3 presents the experiment and concluding remarks are given in Section 4.

2 Materials and Methods

Data Acquisition. The standard brain template was created using MRI data from 15 subjects out of a limited brain MRI dataset. Furthermore, after the rebuilding of the anonymous face model, an extra brain MRI test model was selected and used as cross validation to evaluate our proposed method. The subject MR image set was collected by using a common T1-weighted pulse sequence examined in the Siemens Trio scanner. The data was collected using the following settings: Scan plane is Sagittal section; the field of view (FOV) = 220x220 mm; Pixel Matrix = 256x256; 160 slices, which is interleaved; Slice thickness = 1.2mm, distance factor 50%; Repetition Time (TR) = 2300ms, Echo Time (TE) = 2.94ms; Grappa Factor = 2; Scan time = 5:17.

Anonymous Face Model Creation. Standard brain template construction is the first and most important step in anonymous face modeling. The face of this template is non-recognizable. In medical image processing, registration and normalization are essential preprocesses to build a standard template. During the scalp-skull stripping, an improved level-set algorithm named Canny-edge level-set is proposed and applied.

The completed anonymous face model procedure is described as below, and its frame work is depicted in Figure 1:

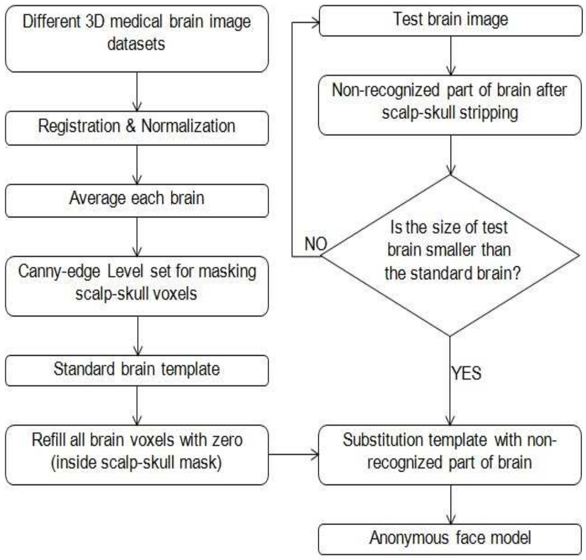

Fig. 1: The completed frame work of anonymous face model.

1. The different datasets were collected to build 3D MR image models as the components of a standard brain template.
2. These component models were bias corrected with registration. After registration, here is the process of normalization. This step can standardize the component models.
3. A simple average processing can be used to build a standard brain template.
4. Next, scalp-skull stripping is applied to a test brain using the Canny-edge level-set algorithm which can get the test inside part of the test brain. The standard brain template is reconstructed by uniting of all voxels with nonzero probability of being scalp-skull as a target brain. All voxels that are inside the scalp-skull mask and have a non-zero probability of being scalp-skull are set to 0.
5. By comparing the size of the inside scalp-skull part of the standard brain with the test brain, if this standard size is bigger than the test brain size, combine the test brain inside skull with this template to build the anonymous face model; if not, the anonymous face model cannot be built. In this paper, we assume this template has a brain volume, which is large enough to contain a test brain. So, the size calculation is skipped in the subsequent experiment.

When the test brain can be combined with the standard brain template, the anonymous face model should be completed.

In theory, a big enough brain image is selected as a target image. Then other brain images are adapted to realize registration and normalization based on the target brain image. Finally, these brains including the target brain are averaged to build the standard brain template.

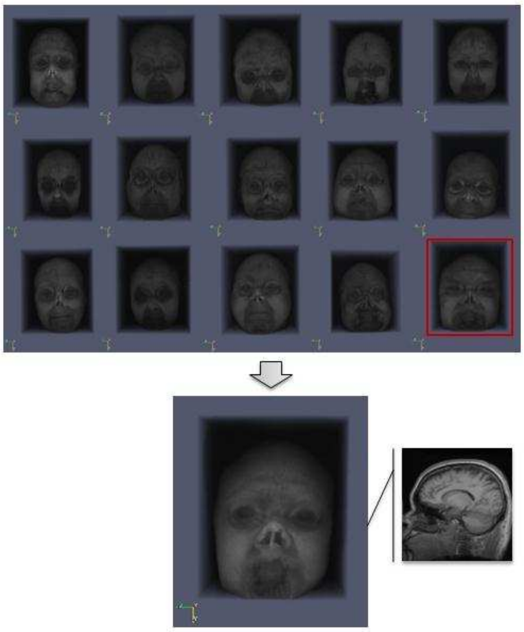

Fig. 2: 3D models: the first three rows contain the component medical brain images of standard brain template and the fourth row shows 3D standard brain template with a 2D image of 70^{th} slice.

Here, we choose fifteen different brain images to build a standard brain, which is shown in Figure 2. One brain marked with a red box is the target brain in this case. In Figure 2, this 3D standard brain template has a similar face to the target brain. The reason is largely due to the number of less recognized brains making an average template. If there are enough brains to make an average process, the result will be a completely non-recognizable face.

B-spline based Deformable Image Registration. This registration method is implemented based on methods described in Rueckert et al [14]. In this particular application we used Normalized Mutual Information (NMI) as a similarity measure. A transformation model is a free-form deformation that is described by a cubic B-Spline defined on a uniformly spaced control point grid (independent of the image data) that covers the moving image. For any point x,y,z part of the moving image the B-Spline transformation is computed from the positions of the surrounding 4x4x4 control points as shown in (1).

$$T(x,y,z) = \sum_{i=0}^{3}\sum_{m=0}^{3}\sum_{n=0}^{3} B_i(u)B_m(v)B_n(w)CP_{i+j,j+m,k+n} \quad (1)$$

where i,j,k represents the index of the control point cell containing the point (x,y,z) and u,v,w are the relative

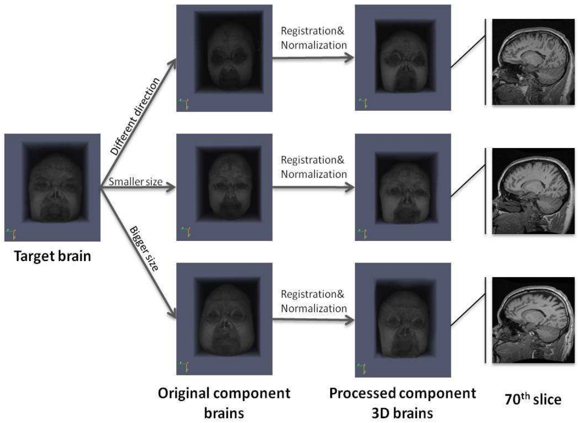

Fig. 3: Pretreatment processes about registration and normalization of component brains in different situations with 2D image of 70^{th} slice.

positions of point (x,y,z) inside that cell in the 3D space. The control point at a specific location is represented by

$$CP_{i+j,j+m,k+n} \quad (2)$$

and the functions B_0, B_1, B_2 and B_3 are the approximations of the third-order polynomials, such as:

$$B_0(t) = \frac{(-t^3+3t^2-3t+1)}{6} \quad (3)$$

$$B_1(t) = \frac{(3t^3-6t^2+4)}{6} \quad (4)$$

$$B_2(t) = \frac{(-3t^3+3t^2+3t+1)}{6} \quad (5)$$

$$B_3(t) = \frac{t^3}{6} \quad (6)$$

The B-Spline transformation T parameters are optimized using a conjugate gradient descent algorithm. The cost function to be optimized is the NMI similarity of the fixed and the moving images. For this implementation, we used a multi-resolution deformation strategy based on multilevel pyramid B-Splines. At each step of the pyramid, the spacing between the control points is increased by a factor of 2 before going to the next step of the registration. Figure 3 illustrates the pretreatment process about registration and normalization of component brains in different situations. This step is used for rotation direction and resizes the 3D brain image.

Level-set Algorithm. Segmentation is typically performed using a mix of automated techniques and semi-automated techniques. With MRI data, segmentation of some structures can be performed just using intensity thresholding. In general, however, segmentation is challenging and requires more sophisticated algorithms and significant human input. Boundary finding segmentation methods, such as Snakes [15], are generally local algorithms that require some feature to be present along the boundary of the object, and gravitate toward that feature. These methods may be sensitive to the starting position and may "leak" through the boundary of the object if the edge feature is not salient enough in a certain region in the image.

Level-set segmentation involves solving the energy-based active contours minimization problem by the computation of geodesics or minimal distance curves [16,17,18]. In this approach, a curve is embedded as a zero level set of a higher dimensional surface [19,20]. The entire surface is evolved to minimize a metric defined by the curvature and image gradient.

In the level-set formulation [19], the propagating front is embedded as the zero level of a time-varying higher dimensional function $\Psi(X,t)$. The level-set function is then evolved under the control of a differential equation. At any time, the evolving contour can be obtained by extracting the zero level-set $\Gamma((X),t) = \{\Psi(X,t) = 0\}$ from the output. The main advantages of using level sets is that arbitrarily complex shapes can be modeled and topological changes such as merging and splitting are handled implicitly.

Level sets can be used for image segmentation by using image-based features such as mean intensity, gradient and edges in the governing differential equation. In a typical approach, a contour is initialized by a user and is then evolved until it fits the form of an anatomical structure in the image. Many different implementations and variants of this basic concept have been published. An overview of the field has been made by Sethian [21].

A generic level-set equation, the (7), was used to update contour lines to the solution Ψ of the partial differential equation [22].

$$\frac{d}{dt}\Psi = -\alpha A(x)\cdot\nabla\Psi - \beta P(x)\,|\,\nabla\Psi\,| + \gamma Z(x)\kappa\,|\,\nabla\Psi\,| \quad (7)$$

where A is an advection term, P is a propagation (expansion) term, and Z is a spatial modifier term for the mean curvature κ . The scalar constants (α,β and γ) weight the relative influence of each of the terms on the movement of the interface.

Canny-edge Level-set Segmentation. The Canny-edge detection method looks for the edges of objects, and can be very useful for images with solid regions, where you only want to vectorise the outlines. The Canny method employs more mathematics than the simple edge detection method, and modifying the settings can improve the results. This method will attempt to find boundaries between poorly defined objects as well as hard edges. Canny has found that the optimal smoothing function for finding edges of a noisy step edge is approximately a Gaussian. Canny defined optimality by defining some reasonable criteria, such as accurate localization and lack of false positives. Hence it is particularly important to reduce the effects of noise before taking a derivative.

The algorithm runs in 5 separate steps:

1. Smoothing: Blurring of the image to remove noise.
2. Finding gradients: The edges should be marked where the gradients of the image has large magnitudes.
3. Non-maximum suppression: Only local maxima should be marked as edges.
4. Double thresholding: Potential edges are determined by thresholding.
5. Edge tracking by hysteresis: Final edges are determined by suppressing all edges that are not connected to a very strong edge.

Skull parts in MR images have a wide intensity variation. In this situation, the skull can not only be seen as a dark strip around the brain, especially in the lower part of the brain where it appears brighter. Hence, the level-set approaches are not effective for extracting skull from its neighboring tissues. For this reason, using canny edge detection in the form of the constructed the skull and applying anatomical constraints seem to be indispensable.

The Canny operation is mainly applied in one-dimensional edge detection. As for the step edges, the shape of optimized edge detection template deduced by Canny is similar to Gaussian function's first order derivative. Utilizing the symmetry and decomposable property of two-dimension Gaussian function, we can easily compute the derivatives on any orientation and convolution of images. Thus, in practical applications we can use Gaussian function's first order differentials as the near-optimized detection operator for step edges. The equation is as follow:

$$G(x,y,\sigma) = \frac{1}{2\pi\sigma^2} = exp\left(-\frac{1}{2\sigma^2(x^2+y^2)}\right) \quad (8)$$

$f(x,y)$denote the image function. The image is smoothed as:

$$g(x,y) = f(x,y)\times G(x,y,\sigma) \quad (9)$$

With the first order differential coefficients of the smoothed image, we obtain the gradient vector form as follows:

$$\begin{bmatrix} g_x(x,y) \\ g_y(x,y) \end{bmatrix} = f(x,y)\times\begin{bmatrix} G_x(x,y,\sigma) \\ G_y(x,y,\sigma) \end{bmatrix} \quad (10)$$

The model value of gradient is $\sqrt{g_x^2(x,y)+g_y^2(x,y)}$, and the orientation angle is arctangent (g_y/g_x) . We will find the maximum along the direction of gradient angle, which are the edge points. If we alter the Gaussian function's σ , we change the size of the Gaussian window.

$$T(x,y,z) = \sum_{i=0}^{3}\sum_{m=0}^{3}\sum_{n=0}^{3} B_i(u)B_m(v)B_n(w)CP_{i+j,j+m,k+n} \quad (11)$$

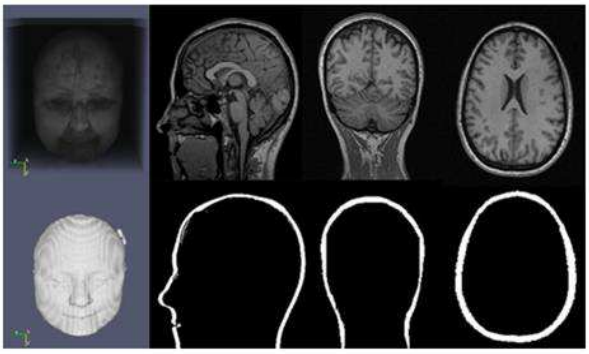

Fig. 4: A sample of Canny-edge Level Set Method: The first row contains the 78th slice of original brain image and the second row contains the same slice of scalp-skull part after applying Canny-edge Level set method.

The curve plane of $\Psi(X,t)$ can be replaced by $g_{xy}(x,y)$ which is the result of canny processing. The curve plane changes into $\Psi(g_{xy}(x,y),t)$. It is then put into the Level Set formula to get the result of a curve evolving with time as follows:

$$\begin{aligned}\frac{d}{dt}\Psi(g_{xy}(x,y),t) = & -\alpha A(x)\cdot\nabla\Psi(g_{xy}(x,y),t) \\ & -\beta P(x) \mid \nabla\Psi(g_{xy}(x,y),t) \mid \\ & +\gamma Z(x)\kappa \mid \nabla\Psi(g_{xy}(x,y),t) \mid \end{aligned} \tag{12}$$

For scalp-skull stripping, Canny-edge level-set algorithm is applied to the test brain images. Figure 4 illustrated an example of the scalp-skull stripping from an original test brain image by using the proposed method.

3 Experiment

Data Acquisition. In order to prove that this anonymous face model cannot change useful original brain information, we make a brain extraction experiment to compare the brain in the original MR image with the brain of the anonymous face model.

In our research, sixteen different medical brain image datasets are prepared. Fifteen medical brain images are used in building the standard brain template as the component medical brain images. Three of these component medical brain images and a new medical brain image are applied as the test brain in the anonymous face model. The experimental procedures can generally be divided into four steps. First, there is a scalp-skull extraction process to get a scalp-skull mask on the 3D standard brain template by using Canny-edge Level set method. Based on standard scalp-skull mask, all voxels that are inside the standard scalp-skull mask are set to 0. Second, segmentation method is applied in the 3D test brain image inside scalp-skull. The scalp-skull part of the test brain is taken off and we can get a non-recognized inside scalp-skull 3D image. The 70th slice of standard brain template on the example is shown in the first row of Figure 5(a). The second row in Figure 5(a) illustrate the brain inside scalp-skull image of a sample brain image after taking off the scalp-skull part with the template in the same slice. The biggest image in Figure 5(a) is the resulting images by combining the test brain with standard brain. Third, by programming, we can combine a series of 2D inside scalp-skull test images with the template one by one. And finally, the anonymous face model is built in 2D combined images. It was necessary to state that the mask calculation is ignored because of the template is assumed to have a big enough brain region. Figure 5(b) show the simple 3D change process from recognized brain to non- recognized brain.

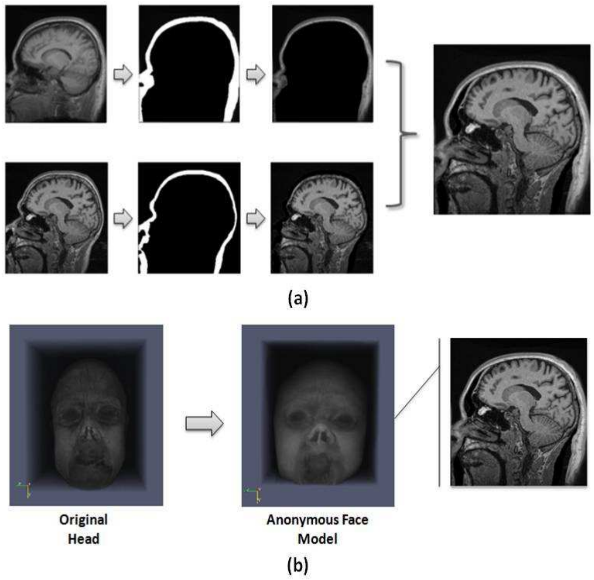

Fig. 5: A Sample of Anonymous Face Model: (a) The first row contains the 70th slice of standard brain template by extracting the scalp-skull part. The second row contains the corresponding slice of a subject inside scalp-skull brain image after stripping the scalp-skull part of the test brain image. (b) The changing process from a recognized brain to a non-recognizable brain.

Results and Validation. After obtaining four anonymous face models, we apply the level set segmentation algorithm to extract the brain image only. Then, we apply the same way to these original brain images in order to validate the conclusion. By obtaining the brain extraction from the original test brain and anonymous face model, we get the number of different pixels that show different intensity value in the corresponding location. According to the number of different pixels, error measurement is the ratio of the different pixel number to the total pixel number in the (13):

$$Error\ measurement = \frac{A}{B} \times 100\% \qquad (13)$$

where A is the number of missed brain voxel and B is the total number of brain voxel. Table 1 shows the results of the brain extraction between the original brain image and their anonymous face models by using the automatic proposed method obtained according to the error measurement. It is clearly observed that error measurement is very small.

Table 1: Error measurement in the brain extraction of the original test brain and anonymous face model.

Different test brain & their anonymous face model	Test brain 1	Test brain 2	Test brain 3	New brain
The total number of missed brain voxel	10310	11654	9855	12436
The total number of brain voxel	1843860	2355373	1533293	1468753
RMS Error measurement (%)	0.56	0.49	0.64	0.85

Here, the new brain image indicated that 0.85% of the pixels difference retained by brain extraction, which is the biggest error measurement in the test cases. Since other test images are the component image of standard brain template, they are easier to match than the new test brain. But these error measurements are still less than 1%. That may imply these error measurement indicate there are differences in the non-brain part, while the real brain information is intact. Because this anonymous face model just replaces the scalp-skull part by using the standard brain template, it does not change the original brain image data.

Overall, we determined that this anonymous face model does an effective job of removing facial features without sacrificing brain tissue. The results of anonymous face model do not interfere with subsequent data processing, and in fact in some cases appears to make subsequent scalp-skull stripping more robust. The method is fully automated and can be scripted to process large quantities of data, making it easy for non-identifiable data to be shared in many medical images processing.

4 Conclusion

Medical image data is highly personal and has a level of individual sensitivity. Increasing access to this data greatly increases privacy risks. Some non-treatment uses of medical data - including quality, research and public health - can be done with data where sufficient patient identifiers have been removed to make it anonymous to the patient. The main concepts of the proposed idea is to construct an anonymous face model to protect the patient's privacy first, and then to make a medical image processing to testify the accuracy by extracting the brain image from the original test brains and their anonymous face models. In anonymous face modeling, there are two important steps for 3D standard brain template building. The first step is to ensure a consistent direction for making the standard brain template. The other step is to match each component brain with the standard brain template, that's because the component brains have different sizes. In brain extraction, the first step is to get a mask result by using Canny-edge level-set algorithm, and then by referring to the mask result, the real brain image data will be extracted.

After applying the anonymous face method to the T1-weighted MR images, to assess the performance of our algorithm, we computed the error measurement, which gives a measure of the difference of the brain extraction results with those obtained from original brain images and their anonymous face model. Our results demonstrated that this method successfully segmented brain images in the anonymous face model with acceptable accuracy for brain segmentation research. In other words, anonymous face model did not appreciably influence the outcome of scalp-skull stripping. Results represented that the automatic method is efficiently robust, to make all the inside scalp-skull tissue changed into a standard template, and does not unduly influence the outcome of the processing methods utilized. Analyses support this method as a viable method to allow data sharing with minimal data alteration within large-scale projects. In the standard brain template building, the similar information can be found in the standard brain template's face. Our future work will focus on improving the standard brain template.

5 Acknowledgement

This paper was supported by research funds of Chonbuk National University partially in 2010. This work was also supported by the National Research Foundation of Korea(NRF) grant funded by the Korea government (MEST) (No. 2012R1A2A2A03).

References

[1] Bruce V, Henderson Z, Greenwood K, Hancock PJB, Burton AM, Miller P. Verification of face identities from images captured on video. Journal of Experimental Psychology: Applied **5**, 339-360 (1999).

[2] Burton AM, Wilson S, Cowan M, Bruce V. Face recognition in poor-quality video: Evidence from security surveillance. Psychological Science **10**, 243-248 (1999).
[3] Rex DE, Shattuck DW, Woods RP, Narr KL, Luders E, Rehm K, Stolzner SE, Rottenberg DA, Toga AW. A meta-algorithm for brain extraction in MRI. Neuroimage **23**, 625-637 (2004).
[4] Fischl B, Salat DH, Busa E, Albert M, Dieterich M, Haselgrove C, van der Kouwe A, Killiany R, Kennedy D, Klaveness S, Montillo A, Makris N, Rosen B, Dale AM. Whole brain segmentation: Automated labeling of neuro-anatomical structures in the human brain. Neuroimage **33**, 341-355 (2002).
[5] Wallois F., Roche-Labarbe N., Aarabi A., Kongolo G., Krim G., Gondry-Jouet C., Abrishami H., Hedou-Roullier V., Dumpelmann M., Grebe R., Localisation de source EEG chez les nouveauxnes prematures: evaluation de l'incertitude due aux parametres du crane, Ann. Cong. of French Clinical Neurobiological Society, France (2005).
[6] Dale AM, Fischl B, Sereno MI. Cortical surface-based analysis. I. Segmentation and surface reconstruction. Neuroimage **9**, 179-194 (1999).
[7] Fennema-Notestine C, Ozyurt IB, Brown GG, Clark CP, Morris S, Bischoff-Grethe A, Bondi MW, Jernigan TL, Fischl B, Segonne F, et al. Quantitative evaluation of automated-skull-stripping methods applied to contemporary and legacy images: Effects of diagnosis, bias correction, and slice location. Human Brain Mapping **27**, 99-113 (2006).
[8] Hahn, HK., Peitgen, H-O. The skull stripping problem in MRI solved by a single 3D watershed transform. MICCAI, LNCS **1935**, 134-143 (2000).
[9] Sled J, Zijdenbos A, Evans A. A nonparametric method for automatic correction of intensity nonuniformity in MRI data, IEEE Transactions on Medical Imaging **17**, 87-97 (1998).
[10] Segonne F, Dale AM, Busa E, Glessner M, Salat D, Kahn HK, Fischl B. A hybrid approach to the skull stripping problem in MRI, Neuroimage **22**, 1060-1075 (2004).
[11] Sandor S, Leahy R.. Surface-based labeling of cortical anatomy using a deformable database, IEEE Transactions on Medical Imaging **16**, 41-54 (1997).
[12] Shattuck DW, Sandor-Leahy SR, Schaper KA, Rottenberg DA, Leahy RM. Magnetic resonance image tissue classification using a partial volume model, Neuroimage **13**, 856-876 (2001).
[13] Fennema-Notestine C, Ozyurt IB, Brown GG, Clark CP, Morris S, Bischoff-Grethe A, Bondi MW, Jernigan TL, Fischl B, Segonne F, et al. Quantitative evaluation of automated-skull-stripping methods applied to contemporary and legacy images: Effects of diagnosis, bias correction, and slice location, Human Brain Mapping **27**, 99-113 (2006).
[14] Rueckert D, Sonoda LI, Hayes C, Hill DL, Leach MO, Hawkes DJ, Nonrigid registration using free-form deformations: Application to breast MR images, IEEE Transactions on Medical Imaging **18(8)**, 712-721 (1999).
[15] Kass M., Witkin A., and Terzopoulos D.. Snakes: Active contour models. International Journal of Computer Vision **1(4)**, 321-331 (1988).
[16] Caselles V., Kimmel R., and Sapiro G.. Geodesic active contours. International Journal of Computer Vision **22(1)**, 61-79 (1997).
[17] Kichenassamy A., Kumar A., Olver P., Tannenbaum A., and Yezzi A.. Gradient flows and geometric active contour models, ICCV, 810-815 (1995).
[18] Malladi R., Sethian J., and Vemuri B.. Shape modeling with front propagation: A level set approach. IEEE Transactions on Pattern Analysis and Machine Intelligence **17(2)**, 158-175 (1995).
[19] Osher S. and Sethian J.. Fronts propagating with curvature-dependent speed: Algorithms based on Hamilton-Jacobi formulation. Journal of Computational Physics **79(1)**, 12-49 (1988).
[20] Baillard C., Hellier P., and Barillot C.. Segmentation of brain 3D MR images using level sets and dense registration. Medical Image Analysis Journal (2000).
[21] Sethian J.A.. Level Set Methods and Fast Marching Methods. Cambridge University Press (1996).
[22] Luis Ibanez, Will Schroeder, Lydia Ng, Josh Cates, The ITK Software Guide Second Edition-Updated for ITK version 2.4, the Insight Software Consortium **9**, (2005).

Ruoyu Du received the Bachelor degree of Biomedical Engineering in the College of Electronics and Information Engineering from the South-central University for Nationalities in the Wuhan of Hubei province, China. And then she received the MS degree in Image Engineering from Chonbuk National University, South Korea. She is currently a Ph.D Student with the Division of Computer Science and Engineering at Chonbuk National University. Her research interests are in the areas of medical image processing, LiDAR research, pattern recognition and EEG research.

Hyo Jong Lee received the MS and Ph. D degrees in computer science from the University of Utah, specialized in computer graphics and parallel processing. He is currently a professor in Division of Computer Science and Engineering and a director of the Center for Advanced Image and Information Technology, Chonbuk National University. His research interests are image processing, medical imaging, visualization, and parallel algorithm.